Available online at www.sciencedirect.com
SCIENCE DIRECT®
Journal of Solid State Chemistry 177 (2004) 3058–3069
JOURNAL OF SOLID STATE CHEMISTRY
http://elsevier.com/locate/jssc

Thermal decomposition and structural reconstruction effect on Mg–Fe-based hydrotalcite compounds

Odair P. Ferreira,[a,*] Oswaldo L. Alves,[a] Daniel X. Gouveia,[b,c] Antonio G. Souza Filho,[b] José A.C. de Paiva,[b] and Josué Mendes Filho[b]

[a] *LQES–Laboratório de Química do Estado Sólido, Universidade Estadual de Campinas-UNICAMP, Instituto de Química, P.O. Box 6154, 13081-970 Campinas, Brazil*
[b] *Departamento de Física, Universidade Federal do Ceará, P.O. Box 6030, 60455–900, Fortaleza-CE, Brazil*
[c] *Centro Federal de Educação Tecnológica-CEFET-Fortaleza-CE, 60040-531, Brazil*

Received 24 November 2003; received in revised form 6 April 2004; accepted 18 April 2004

Available online 25 June 2004

Abstract

The thermal decomposition and structural reconstruction of Mg–Fe-based hydrotalcites (HT) have been studied through thermogravimetric analyses, X-ray powder diffraction (XRD), Fourier transform infrared spectroscopy and Mössbauer spectroscopy. The destruction of the layered structure took place at about 300°C. The broad peaks observed in the X-ray diffractograms suggest that the resultant oxides constitute a solid solution. For samples treated at temperatures higher than 500°C, the formation of the MgO and $MgFe_2O_4$ spinel phases is observed. ^{57}Fe Mössbauer spectroscopy was employed to monitor the Fe chemical environment for the samples annealed at different temperatures (100–900°C). In situ XRD experiments revealed that the HTs start an interlayer contraction at about 180°C. This phenomenon is identified as being due to a grafting process for which the interlamellar anions attach to the layers through a covalent bond. The reconstruction of the HTs was also investigated and its efficiency depends on the thermal annealing temperature and the Mg/Fe ratio. The structure of the reconstructed samples was found to be exactly the same as the parent structure.

Keywords: Layered double hydroxides; Hydrotalcite-like compounds; Pyroaurite; Anionic clays; Thermal decomposition; Mixed oxides; Spinel; Rehydration; Structural reconstruction; *Memory Effect*; Mössbauer spectroscopy; Iron

1. Introduction

Layered double hydroxides (LDHs) or hydrotalcite-like compounds (HTs) have been widely investigated owing to their potential applications as ion exchangers, catalysts and catalyst precursors, pharmaceuticals, UV stabilizers, and adsorbents, among others [1–3]. The general chemical formula of these lamellar solids can be written as $[M^{2+}_{1-x}M^{3+}_x(OH)_2](A^{n-})_{x/n}\cdot mH_2O$ where M^{2+} and M^{3+} are divalent and trivalent cations that occupy the center of $[M^{2+}/M^{3+}](OH)_6$ octahedral units and A^{n-} is an anion. These layered compounds can be viewed as a stacking of positively charged layers (composed of edge-shared octahedral networks) and of negatively charged layers (that both A^{n-} anions and H_2O molecules occupy in a liquid-like configuration).

The HTs are suitable for sorption of anionic species because of their anionic exchange capacity and they have found environmental related applications. These layered materials opened up many possibilities of removing pollutant species from water not only through adsorption on the external surface of the layers but also through an intercalation process. The efficiency of both adsorption and intercalation of anionic species strongly depends on the physical–chemical properties of the HT and mainly on the M^{2+}/M^{3+} ratio that is responsible for the charge in the layers. For instance, HTs are efficient for removing humic substances [4–5], phenols [6], phosphorus [7], chloride [8] and lead from upland surface water [9].

*Corresponding author. Fax: +55-19-37883023.
E-mail addresses: odair@iqm.unicamp.br (O.P. Ferreira), oalves@iqm.unicamp.br (O.L. Alves).
URL: http://www.lqes.iqm.unicamp.br.

0022-4596/$ - see front matter © 2004 Elsevier Inc. All rights reserved.
doi:10.1016/j.jssc.2004.04.030

Among these layered compounds the most studied are the aluminum-based ones. However, the presence of Al has a serious drawback when using these materials in drinking water treatment. Al exposure has been pointed out as a potential risk factor for either the development or the speeding up of the Alzheimer syndrome in humans beings [10]. Considering this scenario, the search for new HTs structures, free of toxic metals such as Al, and the understanding of their physical chemistry properties are highly desirable. The iron-based HTs appear as very promising candidates and some papers dedicated to the study of synthetic Mg–Fe carbonate-based HTs have been published [11–16].

The HTs also exhibit a striking property termed *memory effect* in which some the products of their thermal decomposition experience a spontaneous structural reconstruction when put in aqueous medium. This phenomenon has been observed in Mg–Al and Zn–Al HTs [17], and it is, particularly, well-known in Mg–Al-based HTs [18–20]. Total reconstruction occurs only in a given temperature range where the thermal decomposition is performed. When thermally decomposed at high temperatures, very stable $M^{III}M^{II}_2O_4$ spinel and $M^{II}O$ phases are formed and the HTs cannot be reconstructed. This ability to reconstruct back to their parent structure makes the HTs suitable materials for producing recyclable filters, thus increasing durability and lowering costs [6–7].

Of very much interest is the step-by-step understanding of decomposition and reconstruction processes of the Mg–Fe-based HTs in order to tailor them with the desired physical–chemical properties. Here, we report on the synthesis, thermal decomposition and reconstruction in aqueous medium of the Mg–Fe HT-like compounds for Mg/Fe = 2 and Mg/Fe = 4 molar ratios. We report a very detailed Mössbauer spectroscopy study, which allowed a profound understanding of how the structure behaves during the thermal decomposition process. In situ X-ray powder diffraction (XRD) experiments indicate that the material experiences an interlayer contraction at about 180°C due to a grafting process in which the carbonate anions attach to the layers. The Fourier transform infrared (FTIR) spectra support this assumption since the vibrational modes of the interlamellar anions split. Such a splitting comes from the symmetry lowering effect where the interlamellar anion loose its D_{3h} when get attached to the layer. The rehydration or reconstruction of the Mg–Fe HTs was also investigated and it was found that its efficiency depends on the thermal annealing temperature and the Mg/Fe ratio. A complete reconstruction was possible for samples treated at 500°C for the Mg/Fe molar ratio equal to 4. Both the overall structure (probed with XRD) and local environment of Fe^{3+} order (probed with Mössbauer spectroscopy) for the reconstructed sample were found to be exactly the same as the parent material. Only partial reconstruction was observed for samples with an Mg/Fe molar ratio equal to 2.

2. Experimental procedure

2.1. Materials

All chemicals (reagent grade, Ecibra) were used as received, without further purification processes. All solutions were prepared with deionized water.

2.2. Preparation of HTs

The LDHs or HT-like anionic clays with Mg/Fe molar ratios equal to 2 (*hereafter Mg2Fe*) and 4 (*hereafter Mg4Fe*) were synthesized by the coprecipitation method at variable pH. An aqueous solution (70 mL) containing 0.1 mol of $Mg(NO_3)_2 \cdot 6H_2O$ and 0.05 and 0.025 mol of $Fe(NO_3)_3 \cdot 9H_2O$, respectively, was added dropwise under vigorous mechanical stirring into 150 mL of NaOH (2.0 mol/L) and Na_2CO_3 (0.1 mol/L). During the synthesis, the temperature was kept at 45 ± 3°C. Once the addition of the nitrates was completed a thick slurry was obtained, which was heated for 2 h at 85 ± 3°C for ageing. The final pH of mother liquor was 8–9 to Mg2Fe and 12–13 to Mg4Fe. The products obtained were isolated by filtration and washed several times with deionized water until pH 7–8. Afterwards, the solids were dried at 60°C for 24 h.

2.3. Thermal treatment of HTs

The thermal treatment of Mg2Fe and Mg4Fe (ca 150 mg) was carried out in the 100–900°C temperature range. All samples were heated in air at 10°C/min and kept at a given temperature for 1 h.

2.4. Rehydration process (memory effect)

The rehydration process or reconstruction of the layered structure was carried out with samples thermally decomposed at 400°C and 500°C. An amount of 50 mg of samples was suspended in 10 mL of Na_2CO_3 (0.1 mol/L) solution and kept under magnetic stirring at room temperature for 48 h. The rehydration products were isolated by centrifugation, washed several times with deionized water, and then dried at 60°C for 24 h.

2.5. Techniques

XRD patterns were obtained with a Shimadzu XRD6000 diffractometer, using Cu$K\alpha$ ($\lambda = 1.5406$ Å) radiation operating with 30 mA and 40 kV. A scan rate of 1°/min was employed. In situ XRD measurements were carried out in the 30–600°C temperature range by

using a high-temperature furnace (HA1001, Shimadzu). Before each measurement, 15 min was used for temperature stabilization. The FTIR spectra were recorded using the KBr pellet technique on a Bomem MB spectrometer in the 4000–400 cm^{-1} wavenumber range. The resolution was better than 4 cm^{-1}. Thermogravimetric analyses (TGA) were carry out using a TA Instruments 50 TGA 2050 in the temperature range 25–970°C with heating rate of 5°C/min in air flow (100 mL/min). Chemical analyses for Mg and Fe were carried out by inductively coupled plasma optical emission spectrometry, using a Perkin-Elmer spectrometer (model Optima 3000DV) after the dissolution of the sample in 0.1 mol/L HCl. Elemental microanalyses (carbon and nitrogen) were carry out using a Perkin-Elmer Model 2400 CHN Analyzer. The Mössbauer measurements were performed at room temperature on powdered samples by using standard transmission geometry and a constant acceleration spectrometer with a radioactive source of ^{57}Co within an Rh host. The spectra analyses were performed by using the Normos fitting routine which makes use of a set of Lorentzians and computes the contribution of each curve to the total absorption spectrum through the least-squares procedure. All the isomer shifts (δ) quoted in this paper are relative to metallic iron (α-Fe).

3. Results and discussion

3.1. Chemical analysis

The results of elemental chemical analysis for Mg, Fe, and C/N ratios are given in Table 1. The Mg/Fe molar ratios of the "as-prepared" sample are close to those of the starting solutions thereby indicating that the coprecipitation step was efficiently carried out.

The C/N ratio values suggest that nitrate and carbonate are counterbalancing the positive charge of the brucite-like sheets. The nitrate anion comes from both the $Fe(NO_3)_3 \cdot 9H_2O$ and $Mg(NO_3)_2 \cdot 6H_2O$ reagents used as precursors. The relative amount of carbonate and nitrate is different in the Mg2Fe and Mg4Fe, being larger for the former composition. The remarkable values of C/N ratios could be related to the synthetic method used (variable pH) and to the small time of ageing. It is known that the single anion HTs are obtained only using specific methods (structural reconstruction and hydrothermal treatment) [21]. The presence of two anionic species in the interlamellar region has also been observed by other authors [22–23].

Table 1
Chemical analysis of as-prepared samples

Sample	Mg^{2+a}	Fe^{3+a}	Mg/Fe[b]	C/N[c]
Mg2Fe	17.65	21.51	1.88	0.57
Mg4Fe	21.53	13.26	3.74	2.98

[a] Mass percentage.
[b] Molar ratio.
[c] Mass percentage ratio.

3.2. Thermogravimetric analysis (TGA)

The thermal behavior of the HTs samples was first investigated through the TGA experiments. The TGA scan results for Mg2Fe and Mg4Fe samples are shown in Fig. 1(a) and (b), respectively.

The Mg–Fe HTs start to loose mass from room temperature up to 600°C but the thermal decomposition clearly consists of two distinct steps. The first step (from 25°C to 170°C) corresponds to the loss of water physisorbed on the external surface of the HTs and to the removal of interlayer water molecules, following the reports by Kovanda et al. [15] and Chmielarz et al. [22], that investigated the thermal decomposition of HTs using mass spectrometry. The Mg2Fe and Mg4Fe lose, respectively, 12.3% and 14.6% of their initial mass in this first step. The second step (from 170°C to 600°C) corresponds to mass losses due to the decomposition of the interlamellar anions and dehydroxylation of the

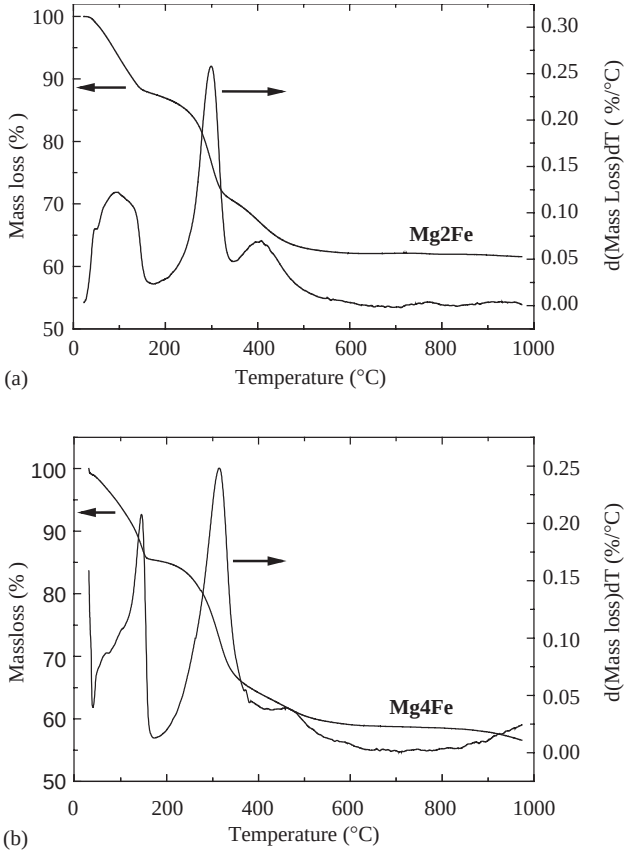

Fig. 1. TGA (left vertical axis) and its derivative (right vertical axis) scans for (a) Mg2Fe, and (b) Mg4Fe samples.

hydroxide layers as well [15,24,25]. The position of the third peak in DTG (mainly the removal of interlamellar anion [22]), occurs in a lower (higher) temperature for Mg2Fe (Mg4Fe). This is attributed to the different amounts of nitrate and carbonate anions in the interlayer space. This behavior should be related to different anion-layer interaction, as we will discuss later in Sections 3.5 and 3.6. The total mass loss up to 600°C was about 40.0% of the initial mass for both Mg2Fe and Mg4Fe samples and no significant mass loss was observed above 600°C.

3.3. X-ray diffraction

The lower trace in Figs. 2(a) and (b) represents the "as-prepared" Mg2Fe and Mg4Fe samples, respectively. The diffractograms for both HTs indicate a high degree of crystallinity of the parent samples and all the diffraction peaks can be indexed to the space group $R\bar{3}m$, thus revealing that the HTs are crystallized in a rhombohedral structure. By analyzing the X-ray diffractograms we obtained that cell parameters are $a = 3.10$ Å (3.10 Å) and $c = 23.61$ Å (23.25 Å) for Mg2Fe (Mg4Fe) sample, which are in agreement with previous reports [12,15]. Vucelic et al. [16] have observed a change in parameter a by changing the Fe content in Mg–Fe HTs. They observed an increase of 0.02 Å when the Mg/Fe molar ratio changes from 2 to 4. In our case, the resolution of our data did not allow us to observe such a small variation. The parameter c depends on Mg/Fe ratio and it was found to be larger for the Mg2Fe sample. An opposite behavior has been observed in Ref. [16]. We attributed this behavior to the nature of the interlamellar space which is composed of carbonate and nitrate whereas in the work by Vucelic et al. [16], the HTs have in the interlayer space only carbonate. We will return to discuss this issue in Sections 3.4 and 3.7. No secondary phases such as $Fe(OH)_3$ and $Mg(OH)_2$, were observed in the X-ray curves for the as-prepared samples. Fig. 2 also shows a sequence of the X-ray diffractograms for several annealing temperatures to which the HTs were submitted.

Remarkable changes are observed for HTs annealed in the 300–500°C temperature range. The well-defined diffraction peaks of the parent samples (lower traces) are replaced by broad peaks, thus indicating a poor long-range ordered phase. These broad peaks suggest a nanocrystalline material with very small nanoparticles or even an amorphous phase. This drastic change in the diffractograms reveals that thermal decomposition of the HT takes place via a highly disordered structure. With a further increase of the temperature of annealing, above 500°C, the broad peaks start to narrow and become more defined for samples treated at 900°C, indicating the presence of crystalline phases. These phases were assigned as MgO (periclase, space group $Fm3m$-JCPDS 45-0946) and $MgFe_2O_4$ (magnesioferrite, space group $Fd3m$-JCPDS36-0398) oxides. Another possible phase to be formed after the thermal decomposition at high temperatures might be maghemite, Fe_2O_3 [15]. It is not possible to make a definite statement whether or not this phase is present in the samples because its Bragg peaks fall at the same angular positions as the MgO and $MgFe_2O_4$ phases. We will return to discuss this issue later, based on Mössbauer measurements.

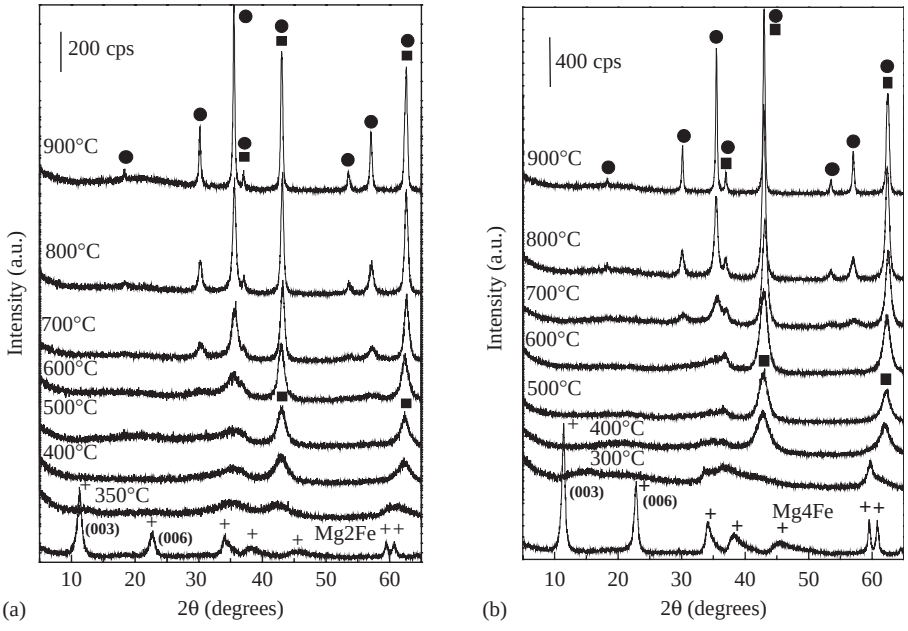

Fig. 2. X-ray diffractograms of the products obtained after the thermal decomposition of (a) Mg2Fe, and (b) Mg4Fe samples. (+) HT; (■) MgO; and (●) $MgFe_2O_4$.

3.4. ^{57}Fe Mössbauer spectroscopy

Although the Fe-based HTs have only Fe^{3+}, their Mössbauer spectra are characterized by an asymmetry, as shown in Fig. 3 for an "as-prepared" Mg2Fe sample. It should be pointed out that this asymmetry is not related to texture effects as one might think. In Fig. 3, the Mössbauer spectra for a Mg2Fe sample recorded for normal incidence ($\theta = 0°$) and in the magic angle geometry ($\theta = 54.7°$) are both depicted.

As can be observed, the spectrum recorded in the magic angle configuration exhibits the same asymmetric profile as the one recorded in the normal incidence, thus indicating that a texture effect contribution to the asymmetry observed in the Mössbauer spectra is negligible. In view of this result, the asymmetry should be attributed to Fe^{3+} positional disorder within the $Fe(OH)_6$ octahedra. This is very likely since the neighbor octahedra present a random distribution of Fe^{3+} and Mg^{2+} and the different neighboring symmetry perturbs the Fe^{3+} differently, thereby suggesting that the Mössbauer spectra should be analyzed considering a distribution of Lorentzian curves to account for the different chemical environments into which Fe^{3+} is inserted. The asymmetry observed in the Mössbauer spectra (shown in Fig. 3) could also be attributed to the presence of Fe^{2+} in the low-spin configuration. This hypothesis, however, is unlikely because in HTs whose divalent cation is Fe^{2+}, this divalent ion is clearly identified in the high-spin configuration [26,27]. Furthermore, these samples containing Fe^{3+} and Fe^{2+} are strongly colored and our samples are not. For completeness, ultra-sensitive chemical analyses of the samples through dichromate (quantitative) and dimethylglyoxime (qualitative) methods were carried out. From both methods no evidence was found of the presence of Fe^{2+} in the Mg–Fe-based HTs.

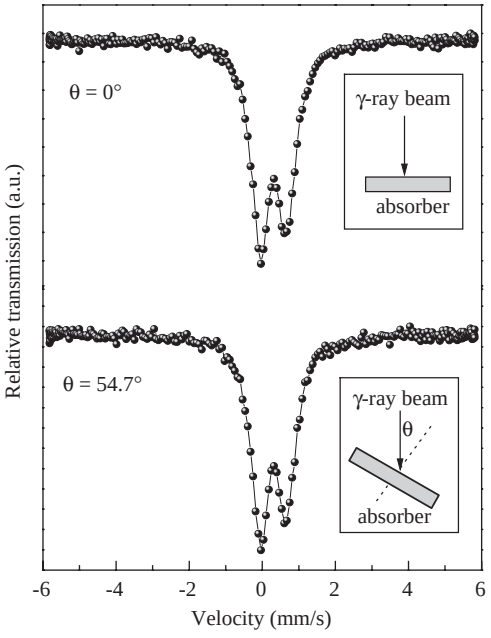

Fig. 3. Mössbauer spectra of the Mg2Fe sample recorded with normal incidence and in the magic angle configuration.

When the Mössbauer spectra, for both Mg2Fe and Mg4Fe samples annealed at different temperatures are analyzed (see Fig. 4), the spectra exhibit a doublet structure in all samples up to a thermal treatment of 700°C. For annealing temperatures higher than 700°C, the spectra start to develop a sextet structure typical of a magnetic configuration. In both samples treated at 800°C the sextets are superimposed on a strong doublet. This doublet is more intense (and the sextet weaker) for the Mg4Fe sample than for the Mg2Fe sample. However, the doublet loses intensity for both samples treated at 900°C although its intensity, relative to the sextet, is higher for the Mg4Fe sample.

All the Mössbauer parameters obtained through the fitting routines are shown in Table 2 for both Mg2Fe and Mg4Fe samples. It is interesting to note that both quadrupole splitting and linewidth are a little larger for samples treated between 300°C and 600°C. This indicates that the samples are getting more disordered in this temperature range due to the decomposition of the layers, in agreement with the X-ray results.

In order to get a more detailed comparison of the magnetic structures, the spectra for samples treated at 800°C and 900°C are shown in Fig. 5. The sextet structure shown in Fig. 5 presents an inhomogeneous lineshape that is characteristic of a magnetic distribution. Due to this fact we used a routine distribution of magnetic fields to fit the spectra.

From the X-ray diffractograms shown in Fig. 2, it is clear that the samples treated at 800°C and 900°C have much better crystallinity. The magnetic distribution used to fit the Mössbauer spectra is not due to structural disorder but is related to the grain size effects, discussed below. According to the X-ray pattern, the magnetic phases formed for samples treated at temperatures higher than 600°C are the spinel $MgFe_2O_4$ and possibly Fe_2O_3. Since both phases have very similar diffraction peak positions, it is very difficult to make a definite assignment on whether or not Fe_2O_3 is present in the samples. However, the $MgFe_2O_4$ spinel structure is the dominant phase. It is known that magnetic nanoparticles exhibit a quadrupole splitting below some critical crystallite size for which the Mössbauer spectrum consists of one doublet that is the signature of a superparamagnetic phase [28]. The inhomogeneous broadening exhibited by the sextets is due to size distribution of the crystallites in the material and the magnitude of the magnetic field B depends on the crystallite size. Although the X-ray measurements point out that the $MgFe_2O_4$ phase starts to form at 600°C, the Mössbauer spectrum typical of a magnetic configuration starts to be observed only for the samples treated at

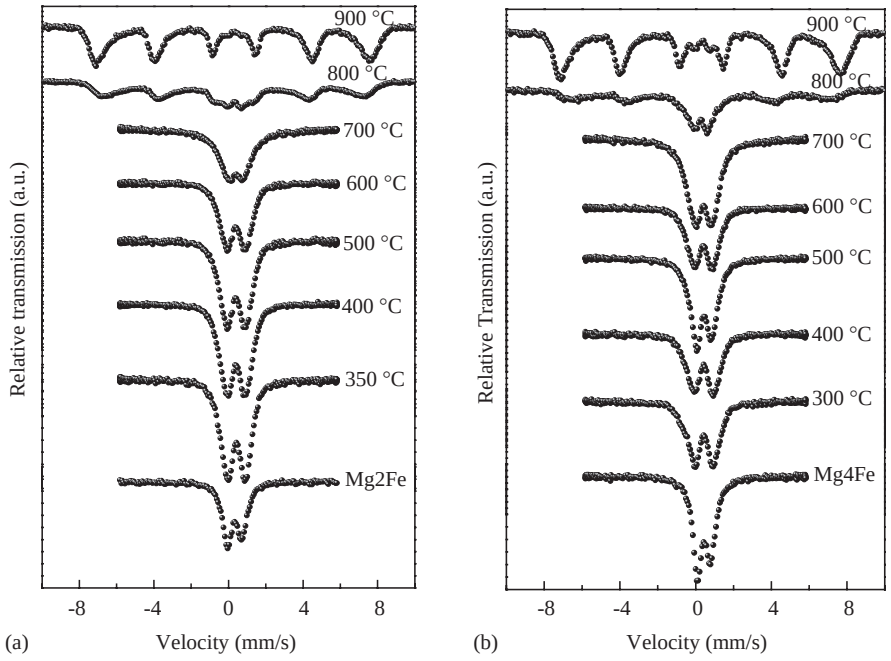

Fig. 4. Mössbauer spectra for (a) Mg2Fe, and (b) Mg4Fe samples obtained by different thermal annealing temperatures.

Table 2
Mössbauer parameters

Sample	Site	Mg/Fe = 2					Mg/Fe = 4				
		ΔQ (mm/s)	δ (mm/s)	B (T)	Γ (mm/s)	p (%)	ΔQ (mm/s)	δ (mm/s)	B (T)	Γ (mm/s)	p (%)
MgFe	Fe^{3+}	0.70	0.39	—	0.29	—	0.65	0.42	—	0.38	—
350/300*	Fe^{3+}	0.85	0.41	—	0.49	—	0.85	0.42	—	0.48	—
400	Fe^{3+}	0.80	0.40	—	0.40	—	0.85	0.41	—	0.40	—
500	Fe^{3+}	0.90	0.39	—	0.37	—	0.70	0.42	—	0.40	
600	Fe^{3+}	0.90	0.39	—	0.37	—	0.80	0.39	—	0.43	—
700	Fe^{3+}	0.85	0.38	—	0.93	—	0.80	0.39	—	0.64	—
800	Fe^{3+}	0.73	0.21	—	—	11.95	0.79	0.19	—	—	35.90
	A	0.09	0.11	28.21	—	39.50	0.21	0.13	21.85	—	19.40
	B	0.00	0.18	43.33	—	48.55	0.04	0.19	42.56	—	44.70
900	Fe^{3+}	0.92	0.17	—	—	4.0	0.88	0.22	—		7.60
	A	0.02	0.17	44.25	—	52.40	0.04	0.18	44.84	—	47.80
	B	0.00	0.18	47.53	—	42.20	0.02	0.18	47.85	—	44.60
ReHT	Fe^{3+}	0.70	0.38	—	0.41	—	0.70	0.43	—	0.40	—

Average splitting quadrupole (ΔQ), average isomer shift (δ), average magnetic hyperfine field (B), linewidth of the distribution (Γ), and the superparamagnetic/magnetic ratio (p) obtained by fitting the spectra of Mg2Fe and Mg4Fe samples treated at different temperatures. ReHT is the product obtained through rehydration of the oxide obtained from a 500°C thermal annealing.

*350 and 300 stand for the temperature thermal annealing for the Mg/Fe = 2 and Mg/Fe = 4, respectively.

800°C. Therefore, the spectra recorded for samples treated at 600°C and 700°C represent the superparamagnetic phase for which the $MgFe_2O_4$ crystallites are quite small. By further increasing the annealing temperature, the crystallite increases and the typical magnetic spectra containing the sextet structure starts to be observed at 800°C for both samples. The growth rate of these $MgFe_2O_4$ crystallites should depend on the Fe content. This hypothesis is supported by the experimental results shown in Fig. 5. When comparing the spectra recorded for Mg2Fe with those recorded for Mg4Fe, it is clear that the crystallite growth rate is lower for the sample with the lower Fe content (Mg4Fe). Even for annealing at 900°C some small crystallites are still present in the samples because the central doublet is visible in spite of its low intensity. By using Scherrer's equation, the average crystallite size evolution from the X-ray results has been estimated and these results are plotted in Fig. 6. In this figure one can observe that the crystallite size for the Mg2Fe sample is higher than for

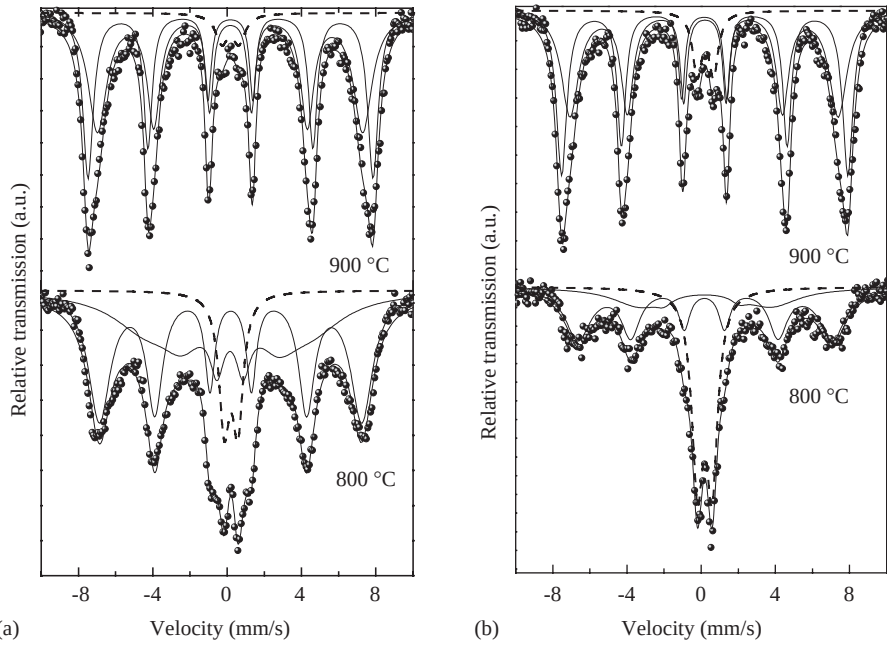

Fig. 5. Mössbauer spectra for samples treated at 800°C and 900°C. (a) and (b) are Mg2Fe and Mg4Fe samples, respectively.

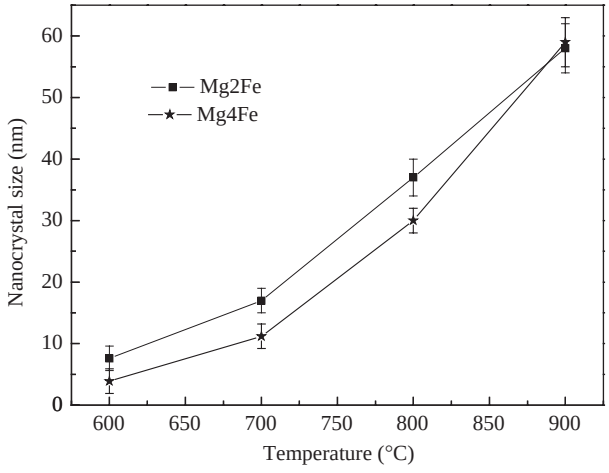

Fig. 6. $MgFe_2O_4$ crystallite size evolutions for Mg2Fe and Mg4Fe samples, determined from XRD data.

the Mg4Fe sample although they both show a tendency to attain the same size when the annealing temperature increases.

The treatment at higher temperatures will coalesce the nanoparticles to form very large (micron-sized) crystallites. The superparamagnetic/magnetic (central doublet/sextets) phase ratio [p (%)] can be evaluated from the Mössbauer spectra. The corresponding results are shown in Table 2 where it is observed that the Mg4Fe sample exhibits higher p values than the Mg2Fe sample, thus indicating that Mg4Fe has smaller crystallites than the Mg2Fe sample.

3.5. *In situ thermal decomposition experiments*

In order to get further insights on the thermal decomposition process of the HT, in situ X-ray measurements were carried out. Similar experiments have been carried out for Mg–Al-based HTs [29]. The temperatures for which the X-ray curves [shown in Fig. 7(a) and (b)] were collected were defined based on the TGA scans depicted in Fig. 1.

The temperature-dependent behavior observed during in situ runs of the Mg2Fe and Mg4Fe samples is in agreement with the X-ray results shown in Fig. 2. On increasing the temperature, the structural modifications of the starting layered structure are clear, resulting in both samples exhibiting X-ray patterns typical of a poor crystalline phase in the 300–500°C temperature range. The behavior of the (003) diffraction peak, which is different for the Mg2Fe and Mg4Fe samples, is remarkable. When the temperature gets close to releasing all the adsorbed and interlayer water (at about 170°C), the (003) diffraction peaks shift towards higher angles, thus indicating a decrease in the interlayer distance. The interlayer distance (d-spacing) and the lattice parameter a were evaluated from the XRD data and their values are listed in Table 3 for different annealing temperatures. The results indicate that the d-spacing is strongly temperature dependent. Conversely, the parameter a does not change (within our experimental resolution) when temperature increases. A similar behavior has been observed by Kanezaki [30].

Both Mg2Fe and Mg4Fe samples experienced an interlayer contraction but it is significantly stronger for

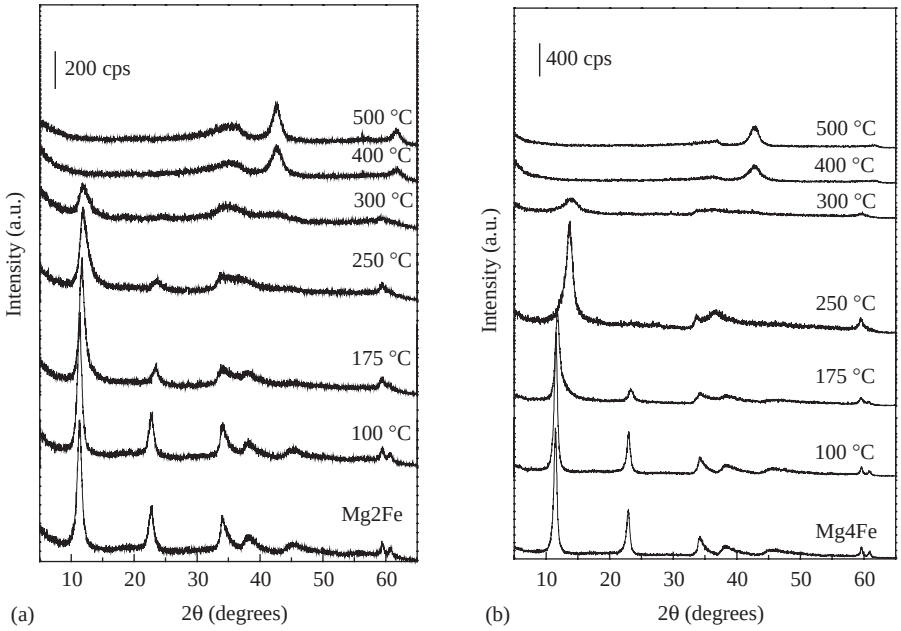

Fig. 7. In situ XRD measurements during the thermal decomposition of (a) Mg2Fe, and (b) Mg4Fe samples.

Table 3
Interlayer distance (*d*-spacing) and cell parameter *a* determined from in situ X-ray data

Temperature (°C)	Mg2Fe		Mg4Fe	
	d-spacing (Å)	*a* (Å)	*d*-spacing	*a* (Å)
25	7.87	3.10	7.75	3.10
100	7.86	3.10	7.70	3.10
175	7.60	3.10	7.54	3.10
250	7.53	3.10	6.51	3.10
300	7.53	—	6.41	—
400	Collapse of layered structure	—	Collapse of layered structure	—

the Mg4Fe sample than for Mg2Fe. This behavior is attributed to the different concentrations of anions species in the interlamellar region. The concentration of anions depends on the Fe content that is responsible for positively charging the layers. In the case of the Mg2Fe sample, there is a high concentration of anions and repulsion between the anionic species competes with interlayer contraction. The interlamellar distance is not strongly reduced, as it is for the sample with a lower anionic concentration (Mg4Fe). Furthermore, the nature of the interlayer space affects the magnitude of the contraction. In order to get a more profound understanding of the interlayer contraction and its connection with anionic concentration and species in the interlamellar region we recall the chemical analysis data listed in Table 1. We found that C/N ratios are 0.57 and 2.98 for Mg2Fe and Mg4Fe samples, respectively. Since the nitrate content is higher than the carbonate content for the Mg2Fe sample, this sample does not experience a drastic layer contraction as it does for the Mg4Fe sample. It is known that for HTs containing nitrate as exchanger anions, this interlayer contraction is very small because these anions do not really attach to the layers via a covalent bond [31]. Then, it is expected that the HT with more nitrate anions would behave like HTs whose exchanger anion is nitrate. This is clearly understood when the behavior of the Mg4Fe sample that has more carbonate than nitrate is analyzed. In this case the interlayer contraction is about 1.2 Å. The interlayer contraction observed for Mg4Fe is due to the grafting of the carbonate anions to the layers thus forming a covalent bond [30,32]. This different interaction level between the anion and layer explains why the releasing of the interlamellar anions (according to TGA results) occurs for the Mg4Fe sample at higher temperature than for the Mg2Fe sample. Therefore, the different behavior of the interlamellar distance during the thermal decomposition is a combination of two effects that are related to the chemical nature of the anions (carbonate vs. nitrate) and to the physical nature of the interlamellar environment (repulsion among the anionic species).

3.6. Infrared spectroscopy

The infrared spectra shown in Fig. 8 for the Mg2Fe and Mg4Fe samples are typical of LDHs and agree well with the typical results reported for HTs [12]. The broad band observed at 3500 cm^{-1} is attributed to the O–H stretching mode (ν_{O-H}) present in the layers and to both adsorbed and interlamellar water. The weak shoulder observed at 3000 cm^{-1} (marked with a downward

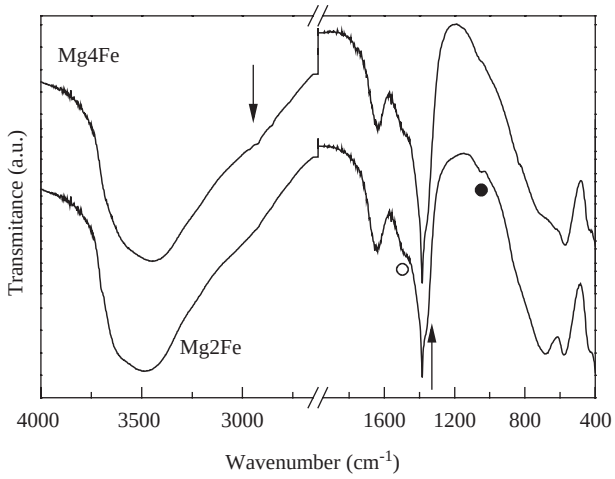

Fig. 8. FTIR spectra of the as-prepared Mg2Fe and Mg4Fe samples.

arrow) is assigned to hydrogen bonds that connect both water and carbonate anions dispersed into the interlamellar regions [33]. The mode at about 1640 cm^{-1} is assigned to HOH deformation (δ_{H-O-H}).

The band observed at 1400 cm^{-1} is composed of two peaks: a sharp peak centered at 1385 cm^{-1} and a broader (marked with an upward arrow) peak centered at 1370 cm^{-1}. The mode located at about 1370 (1385) cm^{-1} is assigned to the v_3 (asymmetric stretching mode) of the carbonate (nitrate) anions. A sharp peak is typical of nitrate anions that exhibit a very strong IR mode [31].

It is well-known that both frequency shifts and splitting of the various modes of molecular species, compared to their free counterparts, are due to the restricted environment into which the anions are placed and to the various hydrogen bonds, thus leading the anionic species (carbonates and nitrates) to experience symmetry lowering effects [31,33]. The evidence for this symmetry lowering phenomenon is the appearance of the shoulder at about 1480 cm^{-1} (marked with an open circle) that is attributed as being due to the splitting of the v_3 of the carbonate. The mode at 1050 cm^{-1} (marked with a solid circle) is attributed to the v_1 mode of the carbonate or of the nitrate that is not infrared active in the D_{3h} symmetry (the configuration of the free anion) [34]. The appearance of both 1480 and 1050 cm^{-1} modes suggests that the anions have a symmetry lower than D_{3h} and that new modes have become active due to both degeneracy breaking and activation of inactive modes. The mode located at about 680 cm^{-1} has been identified as a v_4 mode of the carbonate anions. The remaining bands below 1000 cm^{-1} are due to metal oxygen vibrations.

In situ X-ray measurements have shown that a strong decrease of the interlayer distance (from 7.7 to 6.5 Å) is observed when the Mg4Fe sample was thermally treated at about 250°C. The first attempt to explain such an interlayer contraction would be the removal of both adsorbed and interlamellar water, as was observed in the TGA scans at about 175°C. However, the magnitude of this decrease is not compatible with only water removal and an alternative explanation for this phenomenon is necessary. In order to better understand the chemistry behind the interlayer contraction during heating, we have carried out FTIR measurements focusing the analysis on the spectral region of the anionic species (carbonates and nitrates) (Fig. 9).

From room temperature up to 100°C, only slight spectral changes are observed, thus revealing that, for this thermal annealing temperature range the chemical species present in the interlayer space remain unaltered or undergo only minor changes. In the 175–300°C temperature range, remarkable changes are observed in the IR spectra, i.e., a band at about 1520 cm^{-1} (marked with a downward arrow) and 1350 cm^{-1} (marked with an upward arrow) appear in the spectrum (Fig. 9). These new bands are attributed to a strong interaction of the carbonate anions with the layer, thus drastically modifying the liquid-like configuration of the carbonate anions in the interlayer region. The grafting of the

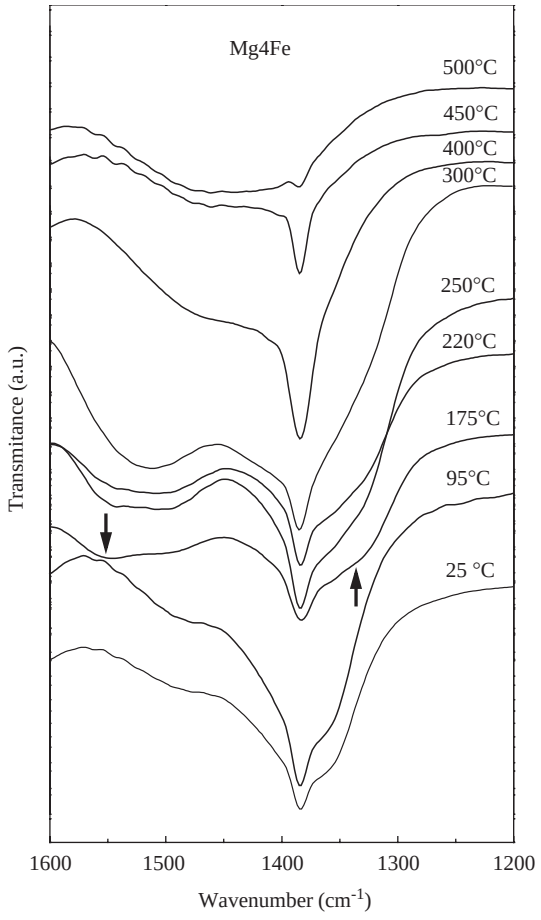

Fig. 9. FTIR spectra of the Mg4Fe sample thermally annealed in the 100–500°C temperature range.

anions with the layer leads to the formation of a new layered phase with an interlayer distance smaller than that observed in the parent sample. This assumption is supported by the in situ X-ray results discussed previously. For temperatures higher than 300°C the band at 1520 cm^{-1} is no longer observed and the v_3 mode drastically loses intensity. These results point out that the anions have a different environment and that the phase formed during the grafting process has been destroyed. Both carbonate and nitrate anions have been released from the solid. X-ray measurements have shown that the crystalline structure formed during the grafting process gets destroyed and the appearance of some broad diffraction peaks could be attributed to the formation of a solid solution. The grafting phenomenon has been observed in other HT-like systems such as Mg–Al [30], Ni–Co and Ni–Fe [32] and Cu–Zn [35]. Even in samples thermally annealed at 500°C, two weak bands located at 1460 cm^{-1} (broad) and at 1385 cm^{-1} (sharp) can be observed that are attributed to the remaining nitrate and carbonate anions. This is in agreement with previous reports that have pointed out that the complete removal of the anionic species occurs only at temperatures higher than 700°C [35]. This is also observed in the TGA scans shown in Fig. 1.

3.7. Rehydration (reconstruction) of the lamellar structure

After the decomposition process, rehydration experiments were carried out in order to reconstruct the lamellar structure. The products of the decomposition for Mg2Fe and Mg4Fe samples obtained with thermal annealing were placed in a carbonate solution. For samples treated at 500°C the starting HT structure was recovered (Fig. 10).

The reconstruction efficiency is not as good for Mg2Fe as it is for Mg4Fe samples. However, all the diffraction peaks present in the "as-prepared" samples were observed in the X-ray pattern for the reconstructed Mg2Fe samples. It is remarkable that the reconstruction of the Mg4Fe sample is so complete that its diffractogram is almost the same as the starting phase, except for the relative intensities of some peaks, linewidths, and also their absolute intensities. This is expected since we have performed powder diffraction measurements and the powder sample distribution on the sample holder differs from sample to sample and some preferential orientation could be favored for different sample preparations. The small differences in linewidths are attributed to the different crystallite size. The interlamellar distance (*d*-spacing) and lattice parameter *a* for the reconstructed HTs were found to be 7.79 Å (7.83 Å) and 3.10 Å (3.10 Å), respectively, for ReHT2 (ReHT4) samples. It should be noted that the *d*-spacing changes for different Mg/Fe ratio being larger for the ReHT4 sample. In the case of reconstructed samples, the interlamellar space is primarily composed of CO_3^{2-} anions and the expansion of *d*-spacing for the lower Fe content sample is consistent with the observations made by Vucelic et al. [16].

We also carried out Mössbauer experiments on the reconstructed samples (see Fig. 11). The Mössbauer data show that the samples treated around 500°C exhibit the largest quadrupole splitting and linewidth (see Table 2) thus supporting the idea that the material during the thermal decomposition is forming a solid solution as we have inferred from the X-ray data. The spectral parameters (see last line in Table 2) were very similar to those determined for the "as-prepared" samples thus indicating that the local chemical environment of the Fe ions has been recovered during the rehydration process.

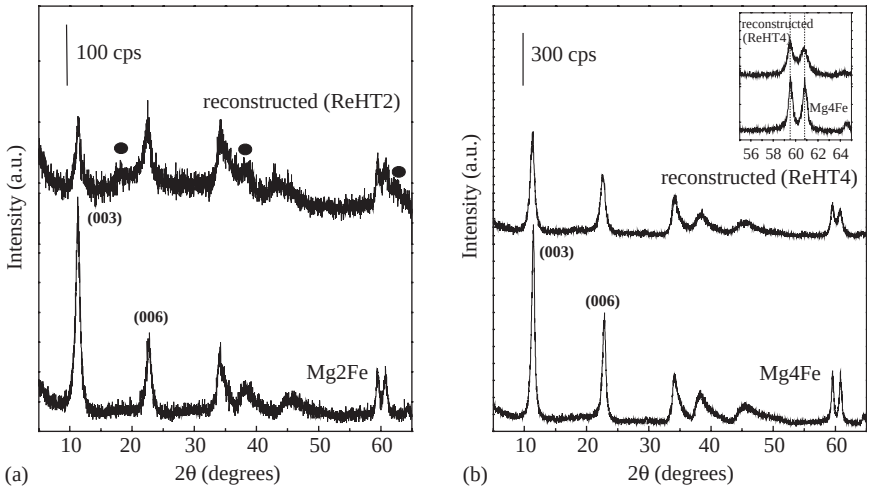

Fig. 10. X-ray diffractograms of the recovered (upper trace) and as-prepared HTs (lower trace) for (a) Mg2Fe and (b) Mg4Fe samples. Reconstructed samples were obtained from products of thermal decomposition at 500°C; (●) $Mg(OH)_2$.

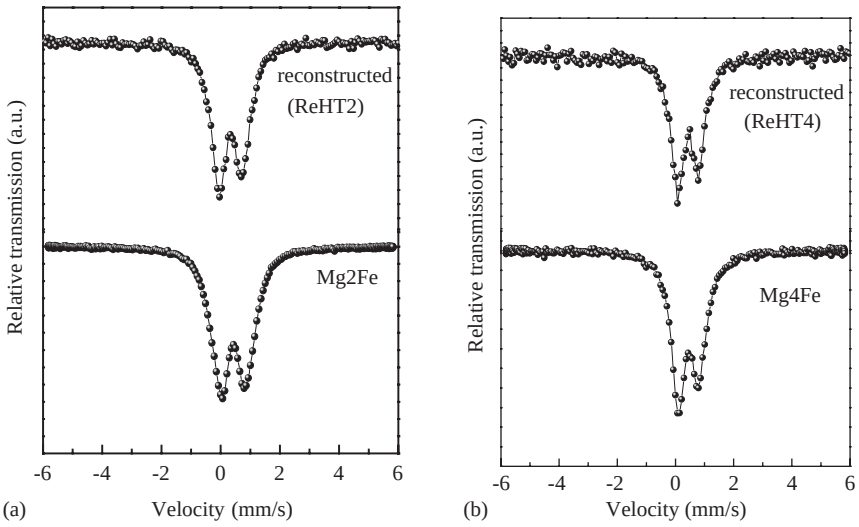

Fig. 11. Mössbauer spectra of the recovered (upper trace) and as-prepared (lower trace) HTs for (a) Mg2Fe, and (b) Mg4Fe samples.

Such a mechanism is possible through a dissolution process of solids formed during the thermal decomposition with a reprecipitation of the double layered hydroxide, similar to what occurs for HTs containing Mg and Al [19]. This assumption is further supported by noting that in the recovered sample obtained from the decomposition process for Mg/Fe = 2 ratio, an isolated phase identified as $Mg(OH)_2$ is observed.

Finally, the reconstruction has been observed only for samples treated at 400°C and 500°C, being more efficient for samples annealed at the later temperature and with an Mg/Fe ratio equal to 4. This is possible because the solid solution formed just after the lamellar structure gets destroyed is a metastable phase and once the system found the appropriate conditions it can reconstruct. When the temperature treatment is distant from the temperature where the lamellar structure was destroyed, forming some stable crystalline phases (mainly the spinel $MgFe_2O_4$), the reconstruction process no longer occurs. For the intermediate configurations where the system does not have the lamellar structure and the energy barrier for starting to nucleate the spinel phase is not yet reached, the HT keeps its structural memory and can totally reconstruct depending on the Fe concentration.

4. Conclusions

We have studied the thermal decomposition and reconstruction processes of Mg–Fe carbonate HTs. The thermal treatment of the HTs at increasing temperatures leads to several structural changes, to occur as follows. At about 180°C, where the interlamellar water release takes place, an interlayer contraction was observed through in situ XRD measurements. This phenomenon was identified as a grafting process in which the carbonate anions attach to the layers. This is confirmed by investigating the local symmetry of the anions through the infrared spectra, which clearly indicate a splitting of the modes as a consequence of a lowered symmetry. By further increasing the temperature treatment the structure gets progressively disordered and, at about 400°C, the layers are destroyed and the oxides form a solid solution. This disorder increase is observed by investigating the chemical environment of the Fe ions through Mössbauer spectroscopy, whose quadrupolar splitting increases when the thermal annealing temperature increases. At higher temperatures (>600°C), the stable MgO and $MgFe_2O_4$ phases start to nucleate and, for samples treated at 900°C, good crystalinity of the samples is observed in the X-ray data. The Mössbauer spectroscopy data reveal the presence of very small nanoparticles of $MgFe_2O_4$ in a superparamagnetic configuration. Sextet spectra typical of the magnetic phase are associated with the spinel $MgFe_2O_4$ phase for samples thermally annealed at 900°C.

Upon rehydration with a carbonate solution, the layered structure is totally recovered for samples treated at 500°C, with an Mg/Fe molar ratio equal to 4. Only a partial reconstruction has been observed for samples with an Mg/Fe molar ratio equal to 2. Samples treated at higher temperatures, where both stable MgO and an $MgFe_2O_4$ phase are formed, do not reconstruct at all. The reconstruction mechanism seems to be via a dissolution process of solids formed during the thermal decomposition with a reprecipitation of the LDH, similar to that proposed for Mg–Al-based HTs. This assumption is further supported by observing that, in the recovered sample with an Mg/Fe = 2 molar ratio, an isolated phase identified in the X-ray diffractogram as $Mg(OH)_2$ is observed. Therefore, when the intermediate

configuration where the system does not yet have the lamellar structure (oxide solid solution) and for which the energy barrier for starting to nucleate MgO and $MgFe_2O_4$ spinel phases is not yet reached, the HTs keep their structural memory and can totally reconstruct, depending on the Fe concentration. It is hoped that, this paper has brought forth new insights for the understanding of both the thermal decomposition and reconstruction processes for Mg–Fe HT and that an assessment of their physical and chemical properties has been achieved.

Acknowledgments

OPF and AGSF acknowledge financial support from the Brazilian agencies CNPq and CAPES (PRODOC grant 22001018), respectively. The authors are indebted to Dr. M.G. da Silva for his valuable help in manipulating the Mössbauer file data format. This is a contribution of PRONEX and Millennium Institute of Complex Materials (IM^2C) programs.

References

[1] F. Cavani, F. Trifirò, A. Vaccari, Catal. Today 11 (1991) 173.
[2] A. De Roy, C. Forano, K. El Malki, J.-P. Besse, in: M.L. Occelli, H.E. Robson (Eds.), Synthesis of Microporous Materials, Vol. 2, Van Nostrand Reinhold, New York, 1992, p. 108.
[3] S.P. Newman, W. Jones, N. J. Chem. 22 (1998) 649.
[4] S. Amin, G.G. Jayson, Water Res. 30 (1996) 299.
[5] Y. Seida, Y. Nakano, Water Res. 5 (2000) 1487.
[6] M.A. Ulibarri, I. Pavlovic, M.C. Hermosín, J. Cornejo, Appl. Clay Sci. 10 (1995) 131.
[7] H.S. Shin, M.J. Kim, S.Y. Nam, H.C. Moon, Water Sci. Technol. 34 (1996) 161.
[8] T. Kameda, Y. Miyano, T. Yoshioka, M. Uchida, A. Okuwaki, Chem. Lett. 10 (2000) 1136.
[9] Y. Seida, Y. Nakano, Y. Nakamura, Water Res. 35 (2001) 2341.
[10] Guidelines for Drinking Water Quality, Recommendations World Health Organization, 2nd Edition, Addendum to Vol. 1, Geneva, 1998, p. 3.
[11] S. Velu, C.S. Swamy, Appl. Catal. A 162 (1997) 81.
[12] J.M. Fernandez, M.A. Ulibarri, F.M. Labajos, V. Rives, J. Mater. Chem. 8 (1998) 2507.
[13] T. Hibino, A. Tsunashima, J. Mater. Sci. Lett. 19 (2000) 1403.
[14] P.S. Kumbhar, J. Sanchez-Valente, J.M.M. Millet, F. Figueras, J. Catal. 191 (2000) 467.
[15] F. Kovanda, V. Balek, V. Dornicak, P. Martinec, M. Maslan, L. Bilkova, D. Kolousek, I.M. Bountsewa, J. Therm. Anal. Calorim. 71 (2003) 727.
[16] W. Vucelic, G.D. Jones, Moggridge, Clays Clay Miner. 45 (1997) 803.
[17] F. Kooli, C. Depege, A. Ennaqadi, A. De Roy, J.-P. Besse, Clays Clay Miner. 45 (1997) 92.
[18] J. Rocha, M. Del Arco, V. Rives, M.A. Ulibarri, J. Mater. Chem. 9 (1999) 2499.
[19] M. Rajamathi, G.D. Nataraja, S. Ananthamurthy, P.V. Kamath, J. Chem. Mater. 10 (2000) 2754.
[20] J.A. van Bokhoven, J.C.A.A. Roelofs, K.P. Jong, D.C. Koningsberger, Chem. Eur. J. 7 (2001) 1258.
[21] R.P. Bontchev, S. Liu, J.L. Krumhansl, J. Voigt, T.M. Nenoff, Chem. Mater. 15 (2003) 3669.
[22] L. Chmielarz, P. Kustrowski, A. Rafalska-Lasocha, R. Dziembaj, Thermochim. Acta 395 (2003) 225.
[23] A. Alejandre, F. Medina, P. Salagre, X. Correig, J.E. Sueiras, Chem. Mater. 11 (1999) 939.
[24] T. Hibino, K. Kosuge, A. Tsunashima, Clays Clay Miner. 44 (1996) 151.
[25] M. Bellotto, B. Rebours, O. Caluse, J. Lynch, D. Bazin, E. Elkaim, J. Phys. Chem. 100 (1996) 8535.
[26] H.C.B. Hansen, S. Guldberg, M. Erbs, C.B. Koch, Appl. Clay Sci. 18 (2001) 81.
[27] A. Gehin, C. Ruby, M. Abdelmoula, O. Benali, J. Ghanbaja, P. Refait, J.M.R. Genin, Solid State Sci. 4 (2002) 61.
[28] R.M. Cornell, U. Schwertmann, The Iron Oxides, VCH, Weinheim, 1996.
[29] F. Millange, R.I. Walton, D. O'Hare, J. Mater. Chem. 10 (2000) 1713.
[30] E. Kanezaki, Inorg. Chem. 37 (1998) 2588.
[31] P. Xu, H.C. Zeng, Chem. Mater. 13 (2001) 4564.
[32] C. Vaysse, L. Guerlou-Demourgues, C. Delmas, Inorg. Chem. 41 (2002) 6905.
[33] F.M. Labajos, V. Rives, M.A. Ulibarri, J. Mater. Sci. 27 (1992) 1546.
[34] M.J. Hernandez-Moreno, M.A. Ulibarri, J.L. Rendon, C.J. Serna, Phys. Chem. Miner. 12 (1985) 34.
[35] I. Melián-Cabrera, M.L. Granados, J.L.G. Fierro, Phys. Chem. Chem. Phys. 4 (2002) 3122.